Ice flow in Greenland for the International Polar Year 2008–2009

Article *in* Geophysical Research Letters · June 2012

DOI: 10.1029/2012GL051634

CITATIONS
200

READS
84

2 authors:

E. Rignot
University of California, Irvine
532 PUBLICATIONS **29,180** CITATIONS
SEE PROFILE

Jeremie Mouginot
University of California, Irvine
142 PUBLICATIONS **8,431** CITATIONS
SEE PROFILE

Ice flow in Greenland for the International Polar Year 2008–2009

E. Rignot[1,2] and J. Mouginot[1]

Received 9 March 2012; revised 2 May 2012; accepted 3 May 2012; published 2 June 2012.

[1] A digital representation of ice surface velocity is essential for a variety of glaciological, geologic and geophysical analyses and modeling. Here, we present a new, reference, comprehensive, high-resolution, digital mosaic of ice motion in Greenland assembled from satellite radar interferometry data acquired during the International Polar Year 2008 to 2009 by the Envisat Advanced Synthetic-Aperture Radar (ASAR), the Advanced Land Observation System (ALOS)'s Phase-Array L-band SAR (PALSAR) and the RADARSAT-1 SAR that covers 99% of the ice sheet in area. The best mapping performance is obtained using ALOS PALSAR data due to higher levels of temporal coherence at the L-band frequency; but C-band frequency SAR data are less affected by the ionosphere. The ice motion map reveals various flow regimes, ranging from patterned enhanced flow into a few large glaciers in the cold, low precipitation areas of north Greenland; to diffuse, enhanced flow into numerous, narrow, fast-moving glaciers in the warmer, high precipitation sectors of northwest and southeast Greenland. We find that the 100 fastest glaciers (v > 800 m/yr) drain 66% of the ice sheet in area, marine-terminating glaciers drain 88% of Greenland, and basal-sliding motion dominates internal deformation over more than 50% of the ice sheet. This view of ice sheet motion provides significant new constraints on ice flow modeling. **Citation:** Rignot, E., and J. Mouginot (2012), Ice flow in Greenland for the International Polar Year 2008–2009, *Geophys. Res. Lett.*, *39*, L11501, doi:10.1029/2012GL051634.

1. Introduction

[2] The Greenland Ice Sheet, with an area of 1.71 million km^2 and an ice volume of 2.85 million km^3, contains enough ice to raise sea level by 7 meters and is principally drained by a set of a few hundred outlet glaciers [*Weidick*, 1995]. Ice velocity varies from a few cm per year near topographic divides to several km per year along fast-moving outlet glaciers. Knowledge of ice velocity is essential to identify areas of fast flow, estimate ice discharge into the ocean, study the temporal and spatial dynamics of ice deformation in relation to climate forcing, analyze the impact of flow rates on ice history, constrain numerical models of ice sheet evolution, and other purposes. Until recently, we had only a partial view at the rate of motion of the ice sheet as a whole. Tremendous progress has been made in the last two decades with the advent of interferometric synthetic-aperture radars (InSAR) which provide an all weather, day and night, high-resolution (100 m), comprehensive mapping of surface motion of land ice at an unprecedented level of accuracy and coverage [*Rignot and Kanagarathnam*, 2006; *Joughin et al.*, 2010]. Despite all the InSAR data that became available since the launch of the European Earth Remote Sensing Satellite-1 in late 1991, there are still large areas in the southern part of the ice sheet where measurements are absent.

[3] Here, we present a nearly complete velocity mosaic of the Greenland Ice Sheet assembled from satellite radar interferometry data acquired during the International Polar Year 2008–2009 by three instruments. We discuss how the map was assembled, the precision of the results, their limitations, the distribution of glacier velocity and the significance of the ice flow structure of the Greenland Ice Sheet revealed by this map.

2. Data and Methodology

[4] We use data collected by 3 sensors aboard satellite platforms managed by 3 space agencies: 1) the European Envisat Advanced Synthetic-Aperture Radar (ASAR), 2) the Japanese Advanced Land Observation System (ALOS)'s Phase-Array L-band SAR (PALSAR) and 3) the Canadian RADARSAT-1 SAR. Envisat ASAR surveyed Greenland in fall 2009, ALOS PALSAR in fall 2009 with a few additional tracks in fall 2007, RADARSAT-1 in fall 2009 with a few additional tracks from fall 2007 and 2008. ALOS PALSAR operates at the L-band frequency, or 1.2 GHz; Envisat ASAR and RADARSAT-1 operate at the C-band frequency, or 5.5 to 5.6 GHz. All data were acquired in horizontal transmit, horizontal receive polarization.

[5] The SAR data used herein are processed from raw format into single look complex images using the GAMMA processor (www.gamma-rs.ch). The data are then combined into radar interferograms after applying a pixel offset correction calculated using a speckle tracking algorithm [*Michel and Rignot*, 1999]. The 3-D vector of ice velocity is calculated assuming surface parallel flow using only the speckle tracking results, i.e., the interferometric phase is not employed. ALOS PALSAR provides the most robust temporal coherence and the vast majority of our ice motion estimates despite a 46-day repeat cycle (Figure 1a). This is because the low-frequency radar signals penetrate deeper in snow and firn [*Rignot et al.*, 2001] and provide a signal that is more robust to surface weathering [*Rignot*, 2008].

[6] Ice velocity products degrade in quality in the interior of Greenland due to the presence of ionospheric perturbations that are comparable in magnitude to the ice motion signal [*Gray et al.*, 2000]. Stripes of ionosphere-induced ice motion error are removed manually or through weighting of multiple track data as explained below. Envisat ASAR and

[1]Department of Earth System Science, University of California, Irvine, California, USA.
[2]Jet Propulsion Laboratory, California Institute of Technology, Pasadena, California, USA.

Corresponding author: E. Rignot, Department of Earth System Science, University of California, 3202 Croul Hall, Irvine, CA 92697, USA. (erignot@uci.edu)

0094-8276/12/2012GL051634

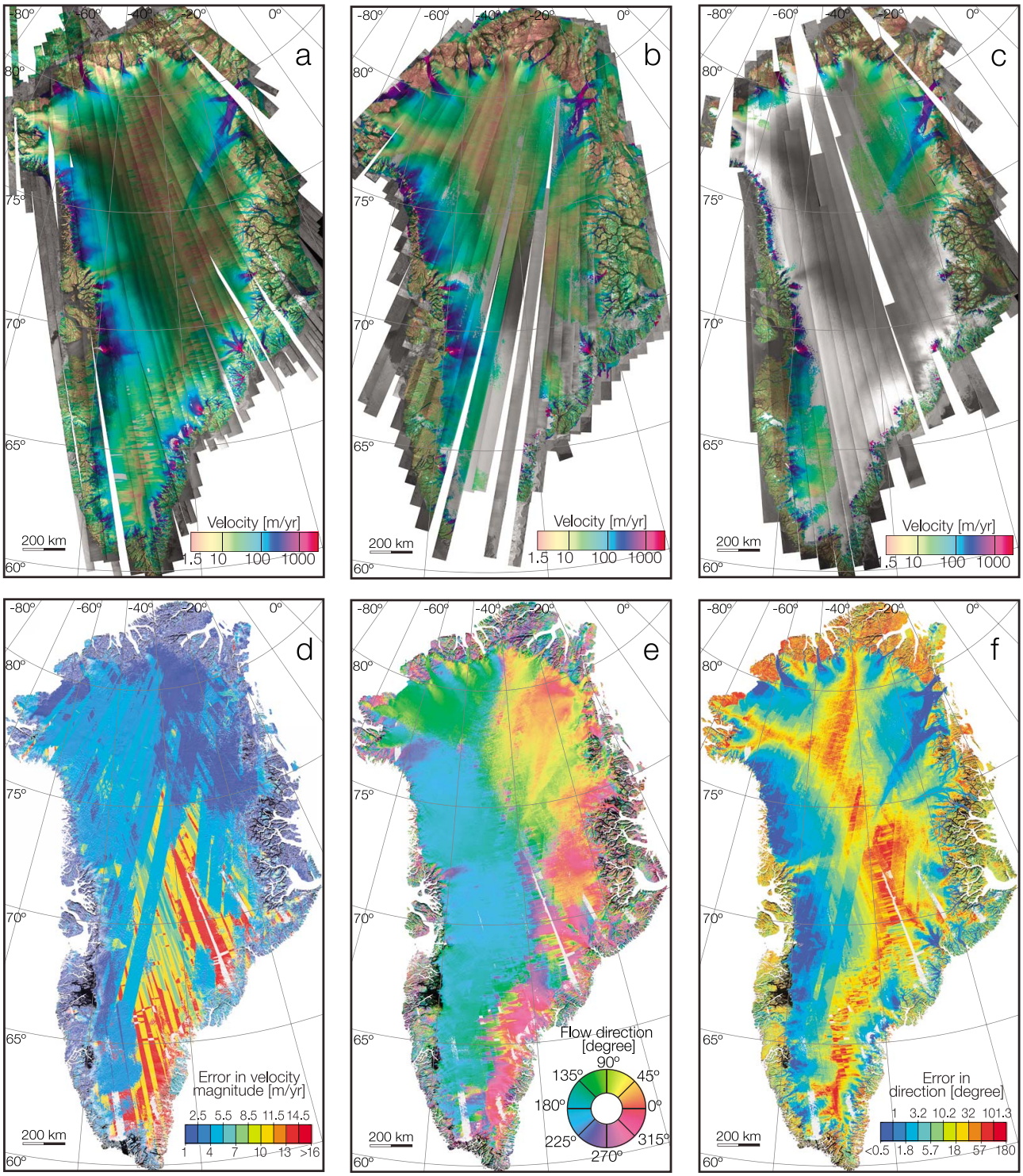

Figure 1. (a) Ground tracks of ALOS PALSAR (L-band, 46-day repeat) (b) ENVISAT ASAR (C-band, 35-day repeat) and (c) RADARSAT-1 (C-band, 24-day repeat) radar interferometry data overlaid on the corresponding ice motion products with a background given by radar brightness; (d) error in flow speed, or velocity magnitude, σ_v, in meters per year; (e) ice flow direction in degrees; and (f) error in flow direction in degrees calculated as $\sigma_v/(2v)$. Color coding in Figures 1a–1c and 1f is on a logarithmic scale.

RADARSAT-1 data are not affected by ionospheric perturbations, which are one order of magnitude lower at C-band (Figures 1b and 1c). C-band data provide high quality estimates in the north, but their long repeat cycle (35-day for ASAR and 24-day for RADARSAT-1) limits signal coherence and the derivation of ice velocity in the south. Exceptions to this rule are rare, e.g., Envisat ASAR in southwest Greenland in fall 2009 (Figure 1c). Residual data gaps exist in areas not surveyed by ALOS PALSAR or where signal coherence is systematically low. ALOS PALSAR

speckle tracking is challenging near the ice fronts of the fastest-moving glaciers because of excessive motion in the 46 days separating consecutive acquisitions. In these areas, we rely on RADARSAT-1 data to complete the mapping (Figure 1b).

[7] The calibration of ice velocity in Greenland is less challenging that in Antarctica [*Rignot et al.*, 2011] because coast-to-coast tracks are abundant, and the coastline includes numerous areas of ice-free rock that provide natural targets of zero motion. Ice and non-ice digital topography is also of better precision than in Antarctica, so that the automatic removal of ice topography during processing of the InSAR data improves data quality and the reliability of control points. In addition to coastal references, we employ ice divides with near-zero surface slope as control points in the ice sheet interior (Figure 2). Ice divides are essential to control the quadratic nature of the interferometer baseline. Our calibration procedure employs no in-situ measurements. For each coast-to-coast track, we estimate an absolute offset and a quadratic baseline calculated in the least-square sense in accord with the imaging geometry of the instrument. From this set of calibrated coast-to-coast tracks, we progressively add neighboring tracks by cross-calibrating them with the reference tracks, effectively using additional control points in the overlapping regions with the reference tracks.

[8] In the presence of multiple tracks from multiple sensors, we calculate a weighted average of the results, with a weight of 1 for C-band products versus 0.2 for L-band products. This procedure maintains a high signal to noise ratio in areas surveyed at C-band and reduces ionospheric noise at L-band. In addition, in areas of fast moving ice ($v >$ 200 m/yr, v is speed), we use a weight of 1 for fall 2009 products, 0.2 for fall 2008 products and 0.05 for year 2007 products. In this manner, our map is mostly representative of conditions in fall 2009. Seasonal fluctuations in velocity of 8 to 10% have been noted on tidewater glaciers [*Rignot and Kanagaratnam*, 2006; *Joughin et al.*, 2008] and summer increases of up to 100 m/yr have been detected on land-terminating glaciers [*Sundal et al.*, 2011]. Our speed estimates may therefore be 1–2% slower than their annual average equivalent.

[9] The precision of velocity mapping varies with sensor, geographic location, processing and time period of analysis. We followed the same approach as for Antarctica [*Rignot et al.*, 2011] to calculate the error in speed, or velocity magnitude, σ_v (Figure 1d). The error ranges from 1 m/yr in regions of high coherence to more than 17 m/yr in areas imaged only with ALOS PALSAR in the presence of significant ionospheric noise. We also calculate the error in flow direction, which is equal to $\sigma_v/(2v)$ (Figure 1e). Errors are less than 0.5° near the coast, which is excellent, to greater than 20° in areas of low speed ($v >$ 10 m/yr). In the proximity of major ice divides, the error exceeds 60° and may reach 180°, i.e., the flow direction is essentially unconstrained.

[10] To perform a zeroth-order analysis of the results, we compare the observed velocity with that calculated for an ice sheet deforming via pure internal deformation. We employ a shallow-ice-approximation model with no sliding, no flow enhancement, a flow law exponent of 3, a driving stress calculated from a digital elevation model of Greenland smoothed over 20 ice thicknesses, ice thickness is from *Bamber et al.* [2001] and the creep parameter A is treated as a constant for the entire ice sheet. In reality, A depends on ice temperature, especially near the bed where most of the internal deformation takes place [*Cuffey and Paterson*, 2010]. An increase in temperature of 4°C changes A by a factor 2. Basal temperature over the majority of the Greenland Ice Sheet varies between its pressure-dependent melting point and −4°C [*Heimbach and Bugnion*, 2009; *Greve*, 2005]. Our deformation velocities should therefore be accurate to within a factor 2 after we best fit the calculated deformation with observations near the topographic divides of north and central Greenland per the spatial domain outlined as a red dotted line in Figure 3a.

3. Results

[11] Major ice motion divides agree well with major topographic divides (Figure 2). At the basin scale, however, in almost all sectors of Greenland, there are subtle differences between the flow direction inferred from InSAR and the flow direction inferred from surface topography. Those differences reflect uncertainties in surface slope (which are largest near the coast) and ice flow direction (which are largest in the interior) but also reflect unsteady ice flow dynamics which needs to be studied in further detail.

[12] Along the flanks of the divides, ice motion is organized in a network of tributaries and glaciers. In the north, relatively few, broad, slow moving glaciers drain the ice sheet, with extensive tributary systems such as Nioghalvfjerdsfjorden, Zachariae Isstrøm and Storstrømmen [*Fahnestock et al.*, 2001] intersped by many sectors of near zero motion, e.g., between Petermann and Ryder, Jungersen and Marie Sophie, Hagen Bræ and Nioghalvfjerdsfjorden, and Storstrømmen and F. Graae glaciers. In contrast, the warmer, higher-precipitation sectors of northwest and southeast Greenland are drained by many, smaller-sized, faster-moving outlet glaciers.

[13] We divide the ice sheet in 6 sectors, nearly equal in size, corresponding to different flow regimes, constrained using surface topography, velocity structure and ancillary data [*Weidick*, 1995]. Table S1 in the auxiliary material lists the location, speed and drainage area of 243 glaciers wider than 1.5 km in size extracted from this map.[1] Speed is reported at the ice front for tidewater and lake-terminating glaciers. For land-terminating glaciers, we report the maximum speed upstream of the ice front since the frontal speed is only representative of the glacier ablation rate, not of its rate of ice transport. The fastest-moving glaciers are Jakobshavn Isbræ (13.2 km/yr), Kangerlussuaq (8.1 km/yr) and Helheimgletscher (7.5 km/yr) in center east, Rink (4.2 km/yr), Store (3.7 km/yr) and Sermeq Kujalleq (3.1 km/yr) in center west, and Daugaard-Jensen (3.5 km/yr) in the east. Many of the other fastest-moving glaciers are rarely discussed in the literature or bare no names: Køge Bugt C and S (5.2 km/yr and 3.0 km/yr) in southeast, two unnamed glaciers in Gyldenløve fjord (3.5 km/yr) in southeast, two unnamed glaciers near Deception Ø (3.3 km/yr) in center east and A.P. Bernstorff Gletscher (3.2 km/yr) in southeast.

[14] Comparing speed with drainage area, we find that 50% of the ice sheet is drained by the top 68 glaciers ($v >$ 1.3 km/yr), 66% with the top 106 glaciers ($v >$ 0.8 km/yr), and 98% for the 243 glaciers listed. Tidewater glaciers drain

[1] Auxiliary materials are available in the HTML. doi:10.1029/2012GL051634.

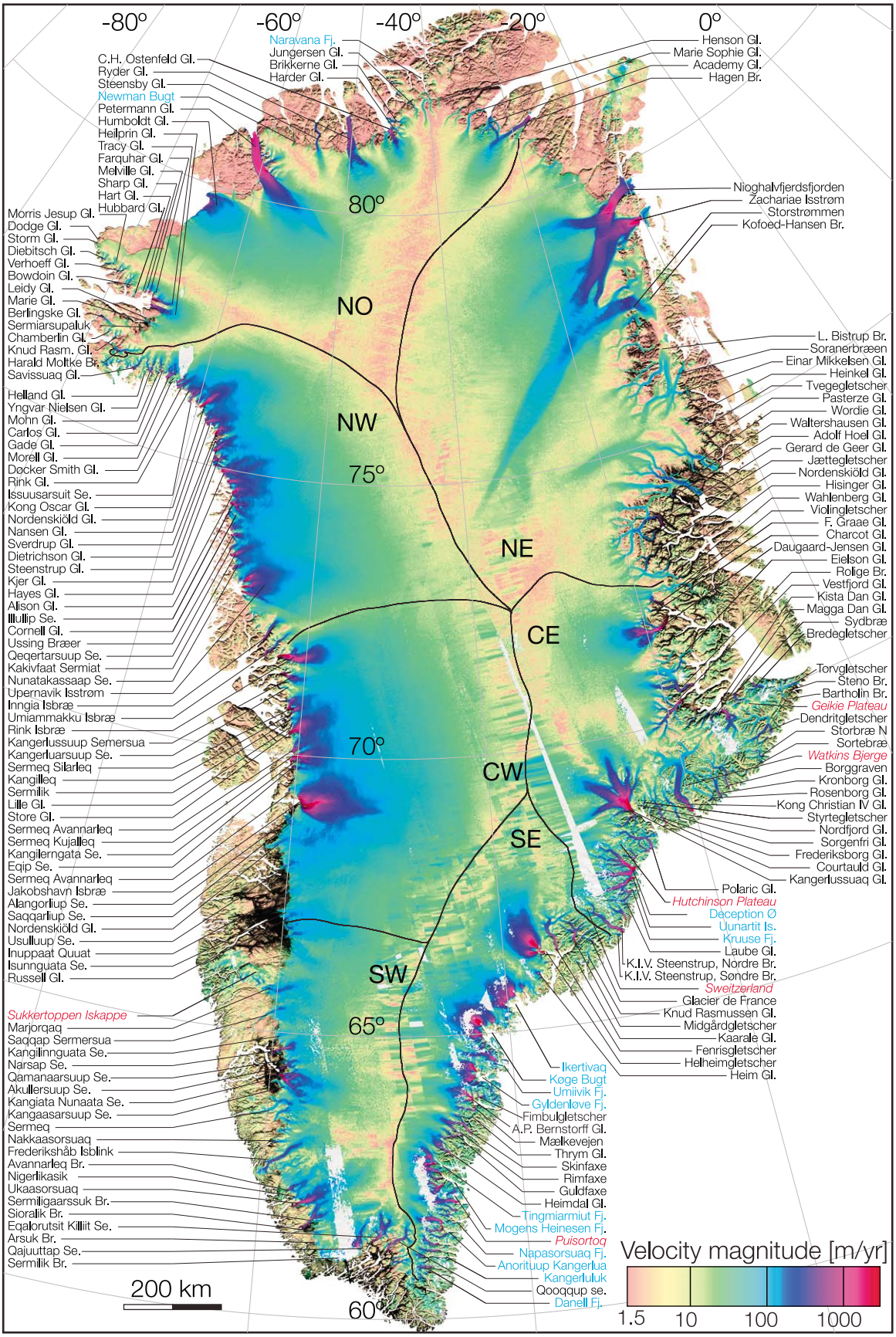
-80°
-60°
-40°
-20°
0°
80°
75°
70°
65°
60°
NO
NW
NE
CE
CW
SE
SW
Naravana Fj.
Jungersen Gl.
Brikkerne Gl.
Harder Gl.
Henson Gl.
Marie Sophie Gl.
Academy Gl.
Hagen Br.
C.H. Ostenfeld Gl.
Ryder Gl.
Steensby Gl.
Newman Bugt
Petermann Gl.
Humboldt Gl.
Heilprin Gl.
Tracy Gl.
Farquhar Gl.
Melville Gl.
Sharp Gl.
Hart Gl.
Hubbard Gl.
Nioghalvfjerdsfjorden
Zachariae Isstrøm
Storstrømmen
Kofoed-Hansen Br.
Morris Jesup Gl.
Dodge Gl.
Storm Gl.
Diebitsch Gl.
Verhoeff Gl.
Bowdoin Gl.
Leidy Gl.
Marie Gl.
Berlingske Gl.
Sermiarsupaluk
Chamberlin Gl.
Knud Rasm. Gl.
Harald Moltke Br.
Savissuaq Gl.
L. Bistrup Br.
Soranerbræen
Einar Mikkelsen Gl.
Heinkel Gl.
Tvegegletscher
Pasterze Gl.
Wordie Gl.
Waltershausen Gl.
Adolf Hoel Gl.
Gerard de Geer Gl.
Jættegletscher
Nordenskiöld Gl.
Hisinger Gl.
Wahlenberg Gl.
Violingletscher
F. Graae Gl.
Charcot Gl.
Daugaard-Jensen Gl.
Eielson Gl.
Rolige Br.
Vestfjord Gl.
Kista Dan Gl.
Magga Dan Gl.
Sydbræ
Bredegletscher
Helland Gl.
Yngvar Nielsen Gl.
Mohn Gl.
Carlos Gl.
Gade Gl.
Morell Gl.
Døcker Smith Gl.
Rink Gl.
Issuusarsuit Se.
Kong Oscar Gl.
Nordenskiöld Gl.
Nansen Gl.
Sverdrup Gl.
Dietrichson Gl.
Steenstrup Gl.
Kjer Gl.
Hayes Gl.
Alison Gl.
Illullip Se.
Cornell Gl.
Ussing Bræer
Qeqertarsuup Se.
Kakivfaat Sermiat
Nunatakassaap Se.
Upernavik Isstrøm
Inngia Isbræ
Umiammakku Isbræ
Rink Isbræ
Kangerlussuup Semersua
Kangerluarsuup Se.
Sermeq Silarleq
Kangilleq
Sermilik
Lille Gl.
Store Gl.
Sermeq Avannarleq
Sermeq Kujalleq
Kangilerngata Se.
Eqip Se.
Sermeq Avannarleq
Jakobshavn Isbræ
Alangorliup Se.
Saqqarliup Se.
Nordenskiöld Gl.
Usulluup Se.
Inuppaat Quuat
Isunnguata Se.
Russell Gl.
Torvgletscher
Steno Br.
Bartholin Br.
Geikie Plateau
Dendritgletscher
Storbræ N
Sortebræ
Watkins Bjerge
Borggraven
Kronborg Gl.
Rosenborg Gl.
Kong Christian IV Gl.
Styrtegletscher
Nordfjord Gl.
Sorgenfri Gl.
Frederiksborg Gl.
Courtauld Gl.
Kangerlussuaq Gl.
Polaric Gl.
Hutchinson Plateau
Deception Ø
Uunartit Is.
Kruuse Fj.
Laube Gl.
K.I.V. Steenstrup, Nordre Br.
K.I.V. Steenstrup, Søndre Br.
Sweitzerland
Glacier de France
Knud Rasmussen Gl.
Midgårdgletscher
Kaarale Gl.
Fenrisgletscher
Helheimgletscher
Heim Gl.
Sukkertoppen Iskappe
Marjorqaq
Saqqap Sermersua
Kangilinnguata Se.
Narsap Se.
Qamanaarsuup Se.
Akullersuup Se.
Kangiata Nunaata Se.
Kangaasarsuup Se.
Sermeq
Nakkaasorsuaq
Frederikshåb Isblink
Avannarleq Br.
Nigerlikasik
Ukaasorsuaq
Sermiligaarssuk Br.
Sioralik Br.
Eqalorutsit Killiit Se.
Arsuk Br.
Qajuuttap Se.
Sermilik Br.
Ikertivaq
Køge Bugt
Umiivik Fj.
Gyldenløve Fj.
Fimbulgletscher
A.P. Bernstorff Gl.
Mælkevejen
Thrym Gl.
Skinfaxe
Rimfaxe
Guldfaxe
Heimdal Gl.
Tingmiarmiut Fj.
Mogens Heinesen Fj.
Puisortoq
Napasorsuaq Fj.
Anorituup Kangerlua
Kangerluluk
Qooqqup se.
Danell Fj.
200 km
Velocity magnitude [m/yr]
1.5
10
100
1000

Figure 2

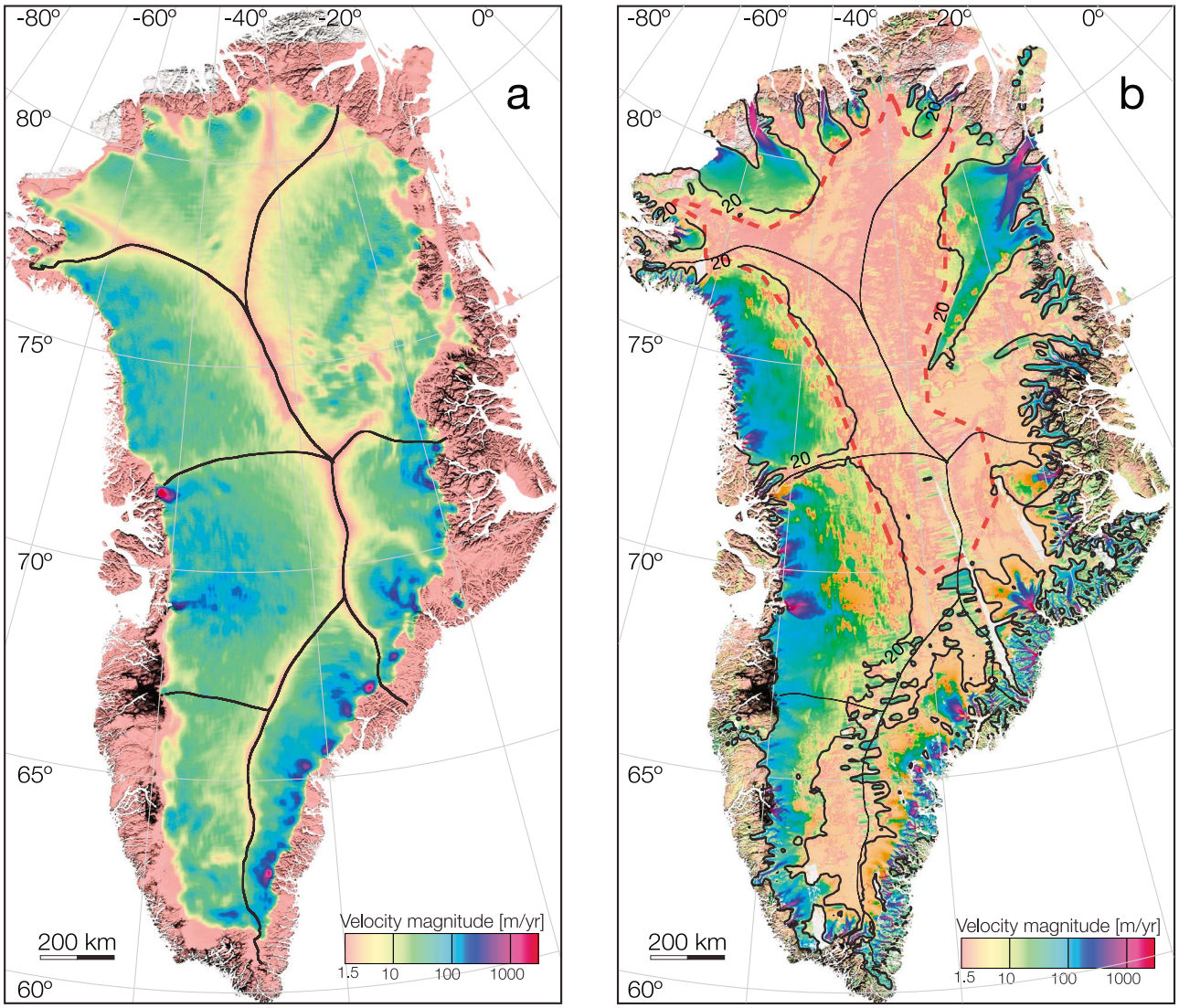

Figure 3. (a) Ice velocity calculated for internal deformation only using an ice rigidity of A = 1.2 10^{-24} s^{-1} Pa^{-3}; and (b) absolute difference between observed and modeled velocity on the same scale as in Figure 2. Black lines are ice divides for 6 subregions discussed in the text and auxiliary material. The red dotted line delineates the area over which model fitting was performed to optimize A and which is equivalent to about one quarter of Greenland in area.

88% of the ice sheet in area and are therefore the dominant type of glacier in Greenland.

[15] The fastest glaciers in the north are Tracy, Heilprin and Petermann, but Tracy and Heilprin drain disproportionately small areas (2,967 and 8,760 km^2 versus 73,817 km^2 for Petermann), which indicates that they flow well above equilibrium conditions. Humboldt is the widest glacier (94 km) with frontal speeds ranging from 0 to 0.5 km/yr. North of C.H. Ostenfeld Gl., the drainage catchments are small. Toward the east, Academy and Hagen Bræ originate from a common source. Storstrømmen, L. Bistrup and Kofoed-Hansen Bræ are surge-type glaciers presently in a quiescent phase that drain 84,965 km^2 or 5% of the ice sheet [*Reeh et al.*, 2003]. South of L. Bistrup, the coastline is rugged, most ice flows through narrow, deeply entrenched, land-terminating glaciers that are slow moving, except for F. Graae (1.2 km/yr), Gerard de Geer (0.9 km/yr) and Adolf Hoel (0.3 km/yr). Waltershausen and Wordie originate from a common source that extends an impressive 300 km inland and nearly connects with the source region of the northeast

Figure 2. Ice velocity map of the Greenland Ice Sheet assembled from satellite radar interferometry data from ALOS PALSAR, Envisat ASAR and RADARSAT-1 overlaid on a MODIS mosaic with a logarithmic color scale ranging from brown (no motion) to green, light green, blue and red (fast motion) at 150 m pixel spacing. Black lines are major ice divides [*Weidick*, 1995]. Glacier and fjord names are discussed in the text. Fj. = Fjord (blue), Br. = Bræ, Gl. = Gletscher or Glacier, and Se. = Sermia. Ice cap names are red. Major regions are labeled as NO = North, NE = North East, CE = Center East, SE = South East, SW = South West, CW = Center West, NW = North West. Ice front and coastline positions are from a complete radar mosaic of the ice sheet from year 2009. The blocky structures near the divides in south Greenland are caused by ionospheric noise.

ice stream known to be fueled by a high geothermal flux [*Fahnestock et al.*, 2001].

[16] Farther south, beyond the pro-eminent Daugaard-Jensen and Vestfjord (1.6 km/yr) glaciers, Geikie plateau and Watkins Bjerge form the largest ice cap in Greenland (34,392 km^2) of which one third is drained by a single glacier: Kong Christian IV Gletscher (11,090 km^2, 1.8 km/yr speed). Magga Dan Gletscher drains another 4,156 km^2 at 1.7 km/yr to the north [*Jiskoot et al.*, 2012]. The second largest ice cap is found on Hutchinson Plateau, between Kangerlussuaq and Helheimgletscher, with 17 glaciers flowing above 1 km/yr. Particularly noteworthy are 3 unnamed glaciers coalescing at Deception Ø and Uunartit Island that flow at 3.3 km/yr and drain 13,773 km^2. This area is experiencing a significant mass loss [*Howat et al.*, 2008]. As in the case of Watkins Bjerge, many of these glaciers reach deep into the ice sheet, making the distinction between ice cap and ice sheet [*Weidick*, 1995] hardly justifiable in terms of ice dynamics.

[17] South of Helheimgletscher and the Switzerland plateau, we find the fastest-moving glaciers in Greenland in the wide fjords of Ikertivaq, Køge Bugt, Gyldenløve and A.P. Berndstorff. Køge Bugt C drains an impressive 18,276 km^2 in size. South of these wide fjords, the glaciers share common sources and are slower because they terminate in narrow valleys. Record flow speeds (1.4 to 3 km/yr) resume in the more open Tingmiarmit and Mogens Heinesen fjords. In the southwest, the 5 fastest glaciers as Narsap Sermia (1.4 km/yr), Ukaasorsuaq (2.8 km/yr), Kangiata Nunaata (1.9 km/yr), Qajuuttap Sermia (2.0 km/yr) and Qooqqup Sermia (1.3 km/yr). Qooqqup Sermia has the interesting particularity of terminating in 3 branches, one on land near stagnant, one in a proglacial lake at 260 m/yr and one in the ocean at 1.3 km/yr. The much larger speed of the tidewater branch is illustrative of the drawing power of marine terminating glaciers. Five other southwest glaciers flow above 0.7 km/yr. Such high flow rates were not expected in a region dominated by massive surface ablation. Between Narsap Sermia and Jakobshavn Isbræ, nearly all glaciers are land terminating. Among them, Frederickshåb Isblink has a fast-flowing core that extends more than 100 km inland. The glacier is mostly land terminating but the fast-flowing core points to a lake-terminating branch, which illustrates again the critical role of water-terminating glaciers on ice sheet dynamics. In centre west Greenland, Jakobshavn Isbræ extends more than 300 km inland. In the centre and northwest, fast-moving glaciers are the norm, with major flow ensembles including Store and Sermeq Kujalleq, Rink, the multiple branches of Upernavik Isstrøm, the triplet Hayes, Alison and Illullip Sermia, Nansen and Sverdrup, and the fast-flowing Kong Oscar that extends for more than 100 km inland, probably revealing the presence of a deep trough in basal topography.

[18] Figure 3 compares the observed velocities with internal-deformation velocities. The best data fit with a deviation of ±4 m/yr over an area equivalent to 25% of Greenland flowing at an average speed of 10 ± 6 m/yr is obtained for $A = 1.2 \pm 0.2 \times 10^{-24}$ s^{-1} Pa^{-3}, which corresponds to an ice temperature of −3.8°C [*Cuffey and Paterson*, 2010]. Changing A by a factor 2 does not improve the model fit over the selected domain (Figure 3b). In the southeast, a lower value of A corresponding to a temperature of −6.5°C provides a better fit, which suggests lower basal temperature in areas of high accumulation. In any situation for A, the model diverges from observations for $v > 20$ m/yr (Figure 3b), which corresponds to 56% of the ice sheet in area. We conclude that basal-sliding motion dominates over the majority of the ice sheet. Basal-sliding motion becomes dominant within only a couple 100 km of major topographic divides.

4. Discussion

[19] The ice motion map provides a unique, new and comprehensive constraint for ice sheet models over 99% of the ice sheet. In comparison, the mapping of ice thickness is far less comprehensive. Our map identifies the most active glaciers which exert the largest control on ice discharge and therefore should receive the highest priority for ice thickness mapping. The ice velocity data can also be used to calculate ice thickness from mass conservation in areas with little to no thickness data [*Morlighem et al.*, 2011].

[20] The northern sector is the closest analog to East Antarctica in terms of flow pattern, i.e., slow moving, far reaching, coalescent tributaries, aka the northeast ice stream. The glaciers in high-precipitation sectors are more diffuse, narrow and akin to Antarctic Peninsula glaciers or glaciers flowing along the Bakutis Coast, in West Antarctica. We attribute these two broad flow regimes to differences in precipitation, not temperature. Precipitation has two major impacts. One is that glaciers in high-precipitation sectors must flow faster to maintain a state of mass balance. A second impact is the ice sheet thermal regime. In areas of low precipitation, vertical advection of heat is low, the basal layers are more isolated from the cold surface, the temperature differential between surface and bed is large, hence ice near the bed is warmer, formation of melt water is more likely, and sliding may develop sooner along the flanks of topographic divides. Conversely, in areas of high precipitation, cold surface temperatures advect vertically more rapidly, the temperature differential between surface and the bed is lower, making the basal layers colder and less likely to melt. We suggest that higher precipitation and a greater vertical advection of cold from the surface to the deeper layers is probably the main reason why subglacial lakes are abundant in East Antarctica but not in Greenland [*Bell*, 2008]. In north Greenland, an average precipitation of 10 cm/yr, ice thickness of 2 km and geothermal flux of 50 mW/m^2, yield a temperature differential between surface and bed of 34°C if we neglect horizontal advection [*Cuffey and Paterson*, 2011, Figure 9.5]. In northwest Greenland, where precipitation is 5 times greater, the temperature differential should be only 13°C, i.e., ice is colder near the bed and less likely to melt. Tributaries extend farther inland in the north likely as a result of more favorable conditions for basal melt water formation compared to tributaries formed in high-accumulation regions.

5. Conclusions

[21] With the advent of three satellite missions and the coordination of acquisition efforts between four space agencies (ESA, JAXA, CSA and NASA), we assembled the first nearly complete map of ice motion in Greenland. A major improvement of this map compared to prior and recent mappings is the broad utilization of ALOS PALSAR data

acquired at the L-band frequency over the entire ice sheet. While L-band data was known to provide higher coherence levels than C-band data, the level of coherence of the L-band data acquired over 46 day intervals was surprisingly high, especially in areas of continuous, intense surface weathering such as southeast Greenland. This map in combination with other data makes it possible to assess the role and relative importance of various glaciers in controlling ice sheet discharge. A copy of the velocity product is available upon request from the authors.

[22] **Acknowledgments.** The authors thank Joanne Shimada, at JPL, for her assistance in processing RADARSAT-1 data and Anker Weidick, at GEUS, for his thorough review of glacier names employed in this study. This work was performed at the Department of Earth System Science of the School of Physical Sciences, University of California Irvine and at the California Institute of Technology's Jet Propulsion Laboratory under a contract with the National Aeronautics and Space Administration's Cryospheric Science Program.

[23] The Editor thanks Jesse Johnson and an anonymous reviewer for assisting with the evaluation of this paper.

References

Bamber, J. L., R. L. Layberry, and S. P. Gogineni (2001), A new ice thickness and bed data set for the Greenland ice sheet: 1. Measurement, data reduction, and errors, *J. Geophys. Res.*, *106*(D24), 33,773–33,780.

Bell, R. (2008), The role of subglacial water in ice-sheet mass balance, *Nat. Geosci.*, *1*, 297–304.

Cuffey, K., and W. B. S. Paterson (2010), *The Physics of Glaciers*, 4th ed., Academic, Amsterdam.

Fahnestock, M., W. Abdalati, I. Joughin, J. Brozena, and P. Gogineni (2001), High geothermal heat flow, basal melt, and the origin of rapid ice flow in central Greenland, *Science*, *294*(5550), 2338–2342.

Gray, A. L., K. E. Mattar, and G. Sofko (2000), Influence of ionospheric electron density fluctuations on satellite radar interferometry, *Geophys. Res. Lett.*, *27*(10), 1451–1454.

Greve, R. (2005), Relation of measured basal temperatures and the spatial distribution of the geothermal heat flux for the Greenland ice sheet, *Ann. Glaciol.*, *42*, 424–432.

Heimbach, P., and V. Bugnion (2009), Greenland ice-sheet volume sensitivity to basal, surface and initial conditions derived from an adjoint model, *Ann. Glaciol.*, *50*(52), 67–80.

Howat, I. M., B. E. Smith, I. Joughin, and T. A. Scambos (2008), Rates of southeast Greenland ice volume loss from combined ICESat and ASTER observations, *Geophys. Res. Lett.*, *35*, L17505, doi:10.1029/2008GL034496.

Jiskoot, H., D. Juhlin, H. St. Pierre, M. Citterio (2012), Tidewater glacier fluctuations in central East Greenland coastal and fjord regions (1980–2005), *Ann. Glaciol.*, *53*(60), 35–43.

Joughin, I., S. B. Das, M. A. King, B. E. Smith, I. M. Howat, and T. Moon (2008), Seasonal speedup along the western flank of the Greenland ice sheet, *Science*, *320*, 781–783.

Joughin, I., B. Smith, I. Howat, T. Scambos and T. Moon (2010), Greenland flow variability from ice-sheet-wide velocity mapping, *J. Glaciol.*, *56*(197), 415–430.

Michel, R., and E. Rignot (1999), Flow of Glaciar Moreno, Argentina, from repeat-pass Shuttle Imaging Radar images: Comparison of the phase correlation method with radar interferometry, *J. Glaciol.*, *45*(149), 93–100.

Morlighem, M., E. Rignot, H. Seroussi, E. Larour, H. Ben Dhia, and D. Aubry (2011), A mass conservation approach for mapping glacier ice thickness, *Geophys. Res. Lett.*, *38*, L19503, doi:10.1029/2011GL048659.

Reeh, N., J. J. Mohr, S. N. Madsen, H. Oerter, and N. Gundestrup (2003), Three-dimensional glacier surface velocities of Storstrømmen glacier derived from radar interferometry and ice-sounding radar measurements, *J. Glaciol.*, *49*(165), 201–209.

Rignot, E. (2008), Changes in West Antarctic ice stream dynamics observed with ALOS PALSAR data, *Geophys. Res. Lett.*, *35*, L12505, doi:10.1029/2008GL033365.

Rignot, E., and P. Kanagaratnam (2006), Changes in the velocity structure of the Greenland Ice Sheet, *Science*, *311*, 986–990.

Rignot, E., K. Echelmeyer, and W. Krabill (2001), Penetration depth of interferometric synthetic-aperture radar signals in snow and ice, *Geophys. Res. Lett.*, *28*(18), 3501–3504.

Rignot, E., J. Mouginot, and B. Scheuchl (2011), Ice flow of the Antarctic Ice Sheet, *Science*, *333*, 1427–1430.

Sundal, A. V., A. Shepherd, P. Nienow, E. Hanna, S. Palmer, and P. Huybrechts (2011), Melt-induced speed-up of Greenland ice sheet offset by efficient subglacial drainage, *Nature*, *469*, 521–524.

Weidick, A. (1995), *Satellite Image Atlas of the Glaciers of the World: Greenland*, edited by R. S. Williams and J. Ferrigno, *U.S. Geol. Surv. Prof. Pap.*, *1386-C*, 153 pp.